

MIT Open Access Articles

Precision positioning using a novel six axes compliant nano-manipulator

The MIT Faculty has made this article openly available. **Please share** how this access benefits you. Your story matters.

Citation: Akbari, Samin, and Tohid Pirbodaghi. "Precision Positioning Using a Novel Six Axes Compliant Nano-Manipulator." *Microsystem Technologies* (2016): n. pag.

As Published: <http://dx.doi.org/10.1007/s00542-016-2931-2>

Publisher: Springer Berlin Heidelberg

Persistent URL: <http://hdl.handle.net/1721.1/105932>

Version: Author's final manuscript: final author's manuscript post peer review, without publisher's formatting or copy editing

Terms of Use: Article is made available in accordance with the publisher's policy and may be subject to US copyright law. Please refer to the publisher's site for terms of use.



Precision positioning using a novel six axes compliant nano-manipulator

Samin Akbari¹ · Tohid Pirbodaghi¹

Received: 16 March 2016 / Accepted: 28 March 2016
© Springer-Verlag Berlin Heidelberg 2016

Abstract In this paper, a novel micro-scale nano-manipulator capable of positioning in six degrees of freedom (DOF) is introduced. Undesired deflections, while operating in a specific DOF, are restricted by the aid of distinctive design of flexure hinges and actuators' arrangements. The compliant mechanism is actuated by thermo-electro-mechanical actuators, as they could be integrated and exert large forces in a nanometer resolution. The actuators are bidirectional capable of applying force in both transverse and longitudinal directions. Performance of the two degrees of freedom actuator is thoroughly explored via numerical and analytical analyses, showing a good agreement. The workspace and performance of the precision positioner is studied using finite element methods. Finally, identification of forward and inverse kinematic of the nano-manipulator is performed utilizing neural network concept. A well-trained and appropriate neural network can efficiently replace the time-consuming and complex analytical and experimental methods.

1 Introduction

High precision positioning is required in many applications including scanning probe microscopy, photonics,

and nano-imprint lithography (Dash et al. 2015; Hosseini et al. 2016; Sitti and Hashimoto 2000). For instance, in optoelectronic devices, a fiber-to-fiber coupling system is used to couple light from one fiber to another or a laser diode requires to be aligned precisely in at least 5 axes. The conventional passive systems currently used for this purpose are lacking the required precision to align fibers and optical modules (Rubio-Sierra et al. 2005). Traditional positioners containing spherical/revolute joints can only be applied for microscale positioning because of the reduced precision caused by friction or wear in the joints. Moreover, clearance in the traditional joints exceeds the workspace of a nano-positioner (Sutherland et al. 1995; Chen et al. 2003; Trease et al. 2005). Compliant mechanisms based on flexure hinges offer an alternative promising route to achieve nanoscale positioning. They rely on deflection of some or all of their parts to achieve motion and hence, offer many advantages, such as reduction in number of parts, diminished friction and wear, and the need for assembly. Furthermore, the monolithic structure of the flexure-hinged mechanisms facilitates their miniaturization and fabrication in the micro scale by the standard microfabrication processes (Yao et al. 2007; Lai et al. 2005; Chen and Culpepper 2006). However, an elaborate design is required to tackle the complexity of motion of several flexible parts. In this paper, a novel 6 axes nano manipulator using a distinct design of flexure hinges to achieve both in-plane and out of plane positioning is designed. Thermo-electro-mechanical actuator capable of applying force in transverse and longitudinal directions is integrated to achieve six degree of freedom positioning. The performance of the compliant positioner is investigated using finite element method (FEM).

✉ Tohid Pirbodaghi
ptohid@mit.edu
Samin Akbari
sakbari@mit.edu

¹ Mechanical Engineering Department, Massachusetts Institute of Technology, 77 Massachusetts Avenue, Cambridge, MA, USA

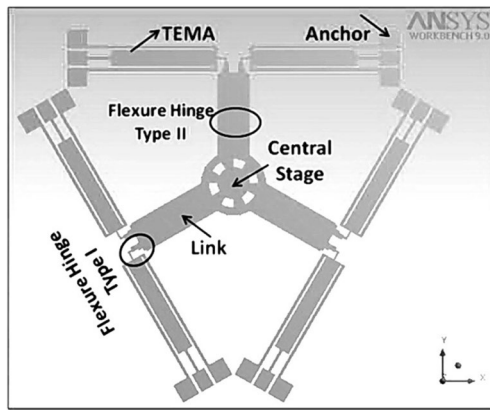


Fig. 1 Schematic of the nano-manipulator

2 Design and modeling of the compliant nano-manipulator

2.1 Conceptual design

The nano-manipulator includes a central stage attached to three links jointed to micro-scaled actuators by flexure hinges. The total structure is fixed to the ground via the actuators, which provide both transverse and longitudinal displacement. Schematic of the compliant mechanism is shown in Fig. 1. Restricting unwanted motions, while operating in a specific DOF, is one of the most challenging topics in designing the nano-positioner. This has been achieved by design and use of certain types of flexure hinges in accompany with distinctive arrangement of actuators.

Two types of flexures are utilized in this compliant mechanism. First type is a simple circular hinge flexure with an out of plane axis of rotation providing in plane deflections. This flexure is used at the junction of actuators to the links. The other type of flexure hinges is created by removing the material from the mid of links and weakening them. Since axis of rotation of this kind of flexures is in-plane, it could provide out of plane motion of the stage.

Forces required to deflect the flexures are applied by actuators. Thermo-electro-mechanical actuators (TEMA) are employed in this nano-positioner, since they could (1) be integrated and fabricated in the micro-scale, (2) deliver nanometer level resolution and (3) are capable of exerting large forces. A novel two DOF and bidirectional actuator is designed and utilized for actuating the compliant manipulator. Performance and analysis of the actuator is thoroughly explored in the next section of this paper.

While TEMA operates in its longitudinal DOF, exerts a normal force to the link deflecting it in the mid, where the out of plane flexure exists. This causes the stage to displace in the out of plane directions. For achieving in plane

displacements, TEMA should operate in its transverse DOF, bending in plane flexures. In this case out of plane flexures remain unchanged, since the translational forces exerted by the actuators cannot supply in plane moment required for deflecting them.

2.2 Study on the performance of the nano-manipulator

Performance of the nano-positioner highly depends on the arrangement of the actuators. In the proposed design, actuators' arrangement has made use of the maximum aptitude of the novel TEMAs for achieving one to six degree of freedom positioning. Examples of positioning of the structure are explained and depicted in Fig. 2.

For Y axis positioning, actuators connected to two oblique links exert normal inward forces while the remained two actuators at the top pull the stage, resulting in positive Y direction motion (Fig. 2b). The advantageous of bidirectionality and distinct arrangements of the actuators in compare with previous researches is clear here. In most of recently designed three DOF micro-manipulators, a multiple of three actuators encircled the center stage, resisting it to displace in in-plane translational DOFs due to their inherent stiffness. Consequently mostly special spring type elements or links have been used deforming and permitting the stage to move in X or Y directions. In this design in contrary with prior designs, operating in the reverse direction of the translational DOF of the novel actuators pulls the stage as well as not resisting anymore.

- For Z axis positioning, all the actuators exert normal forces to links, deflecting the mid-flexures, and displacing the center stage in the Z direction (Fig. 2c).
- For Z axis rotation, three tangential forces are exerted to the links via three of the actuators rotating it in the clockwise Z direction. Similarly, the mirrored actuators could be chosen to achieve counter clock wise rotation (Fig. 2a).

3 Design and analysis of the micro actuator

Thermo-electro-mechanical actuator providing two degrees of freedom is designed to displace the compliant mechanism in both in plane and out of plane directions. This actuator is composed of two thin beams and a thick one connected to the base by a flexure. Beams are fixed at their ends, where voltage is applied. Due to the difference in length and cross-sectional area of beams, their electrical resistance differs resulting in dissimilar heat generated in the device when the voltage applied. Benefiting this principal and applying different voltage arrangements,

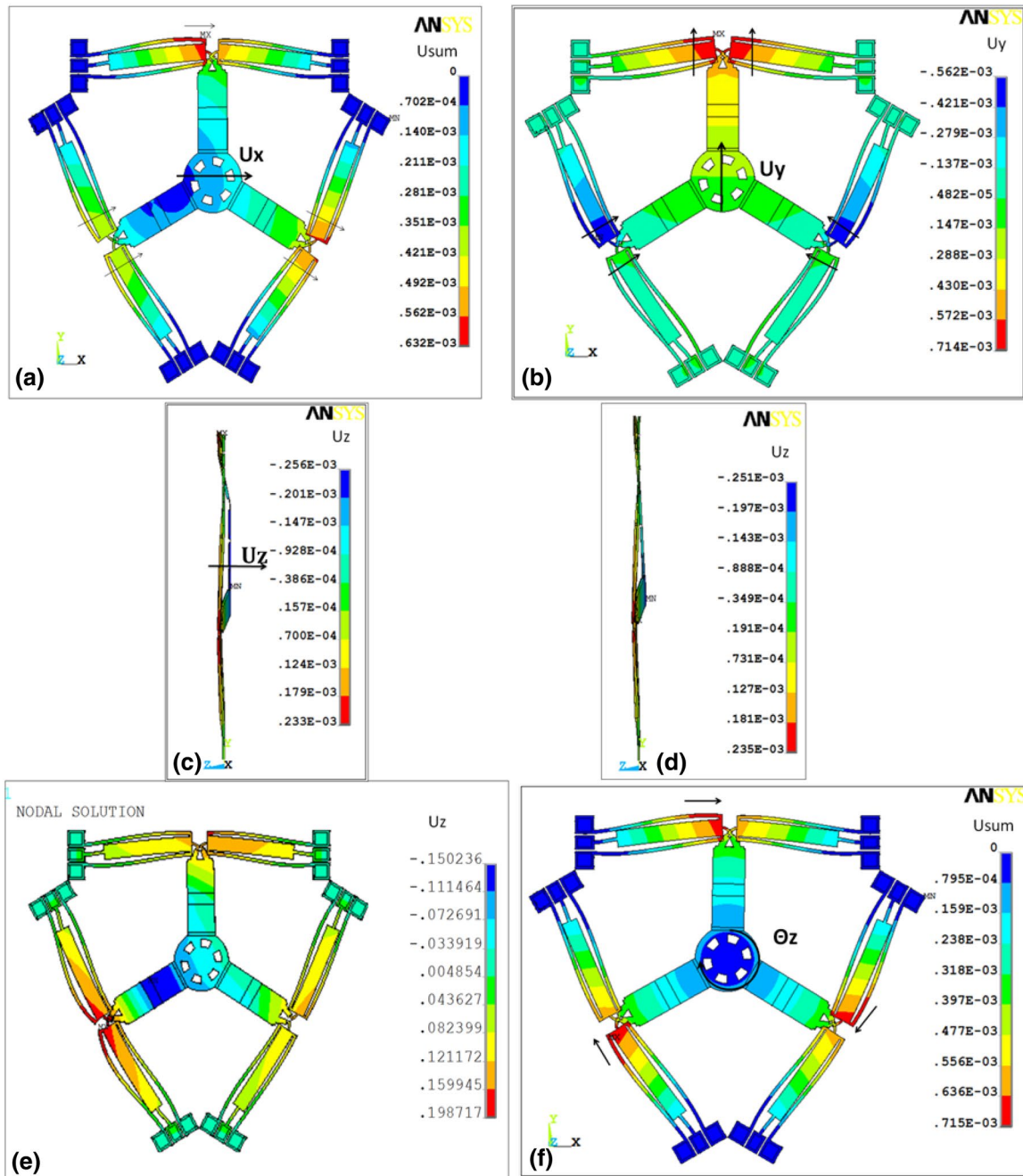


Fig. 2 Examples of positioning; **a** X axis deflection, **b** Y axis deflection, **c** Z axis deflection, **d** X axis rotation, **e** Y axis rotation, **f** Z axis rotation

displacement in translational and longitudinal directions is achieved. In addition, the symmetric design of the actuator has resulted in bi-directionality in the transverse DOF.

When voltage is applied to the left thin driving beam and the remained two voltages kept equal to zero, the current flowed through it, is more than the other beams and consequently the thermal strain induced in it by Joule heating is larger, which bends the structure and results in an X displacement from left to right. Similarly, when the voltage is

applied to the right thin beam the actuator deflects in the X direction from right to left, proving bi-directionality of the device. Figure 3 depicts deflection and temperature profile of the designed thermo-electro-mechanical actuator in its transverse DOF.

The actuator will be able to exert force and supply displacement in its next DOF, while two voltages are applied to both of the thin beams. In this case, the device displaces in the Y direction as indicated in Fig. 4.

Fig. 3 Transverse DOF, **a** voltage, **b** temperature, **c** deflection

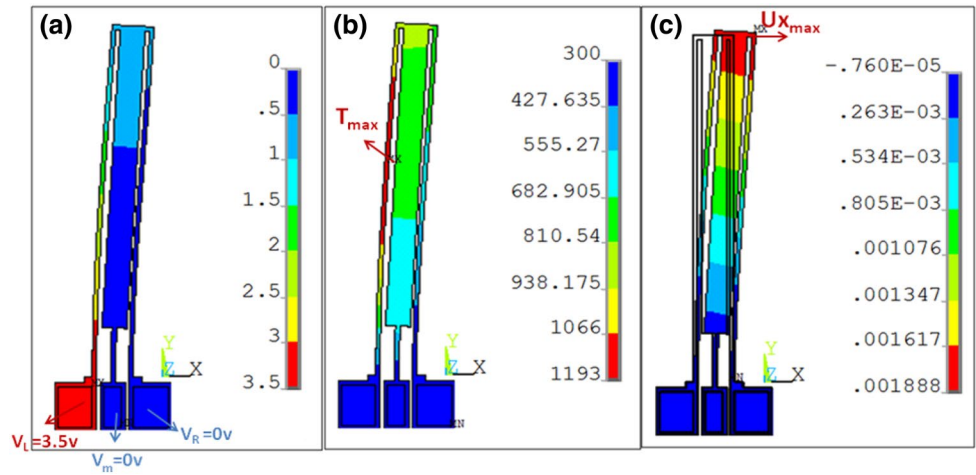
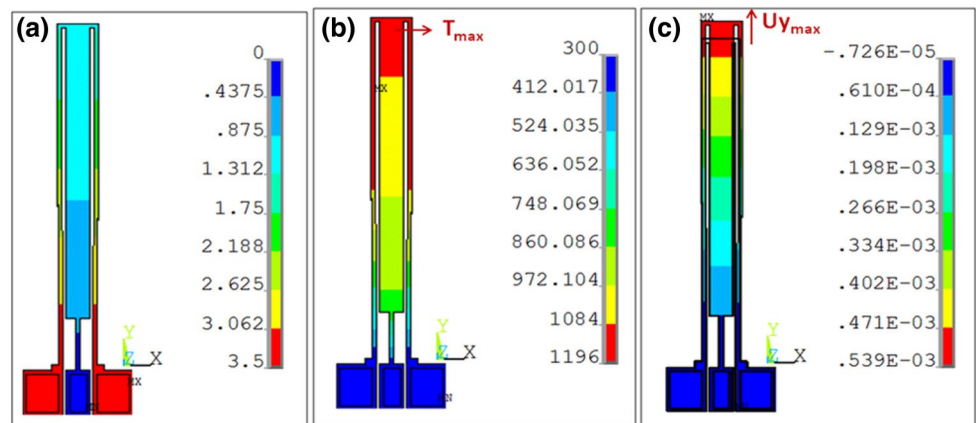


Fig. 4 Longitudinal DOF, **a** voltage, **b** temperature, **c** deflection



In order to verify results obtained via FEM method, analytical analysis of the thermo-electro-mechanical actuator is performed. For this purpose, theoretical electrical, thermal and structural modeling of the new actuator is first given and governing equations are derived.

3.1 Theoretical modeling and analysis of TEMA

In this section, modeling and analysis of thermo-electro-mechanical actuator in each of its DOFs is presented. Analytical and numerical results are then compared with each other that are in good agreement.

Deflection of a TEMA occurs due to different thermal strains induced in its arms by Joule heating. Consequently, to explore performance of the actuator, first, the current flowed in each beam, when voltages are applied, is derived. Next, the temperature distribution in the device is developed enabling to compute the induced thermal strain in each substructure. Finally, using Castigliano theorem, range of motion of the TEMA is obtained.

3.1.1 Electrical analysis

In contrary with the conventional U-beam thermal actuators, the current in this TEMA is not constant through the device and differs in each arm, because three voltage sources exist. Writing the Kirchoff current and voltage laws in the structure, current in each beam is obtained.

$$I_m = \frac{R_3(V_L - V_m) + R_1(V_R - V_m)}{R_1.R_2 + R_2.R_3 + R_1.R_3} \quad (1)$$

$$I_R = \frac{R_1(V_m - V_R) + R_2(V_L - V_R)}{R_1.R_2 + R_2.R_3 + R_1.R_3} \quad (2)$$

$$I_L = \frac{R_2(V_L - V_R) + R_3(V_L - V_m)}{R_1.R_2 + R_2.R_3 + R_1.R_3} \quad (3)$$

where, I_L , I_m and I_R are current flowed in the left, middle and right beams respectively. R_1 , R_2 and R_3 are electrical resistance of each branch of the structure and V_L , V_m and

V_R are voltages applied to the left, middle and right beams respectively.

3.1.2 Thermal analysis

For thermal modeling of the TEMA, first the Biot number, ratio of resistance to conduction with in a solid to resistance to convection-radiation, is evaluated.

$$Bi = \frac{hL}{K} = \frac{100.200.10^{-6}}{157} \cong 10^{-6} \ll 1 \tag{4}$$

where, h is an estimated worst case value of radiation-convection heat transfer coefficient (Culpepper and Anderson 2004). L is length of the driving beam and k is the thermal conductivity coefficient.

For Biot numbers of much less than unity, it is reasonable to assume a uniform temperature distribution across the solid at any time, representing a small temperature gradient in it (Moulton and Ananthasuresh 2001). Therefore, the TEMA is decomposed into three line shape micro-beams; two thin driving beams and one thick beam attached to a flexure.

Now, in order to determine effect of each of the heat transfer modes on TEMA, a lumped mass one dimensional micro-beam, in which a current flowed, is considered.

$$\rho \forall C_p \frac{dT}{dt} = -\varepsilon \cdot \sigma \cdot A_s(T^4 - T_0^4) - k \frac{A_c}{L}(T - T_0) - hA_s(T - T_0) \tag{5}$$

Then the heat transfer via each of convection and radiation respect to conduction in several temperatures is computed. Heat transfer via convection is less than 0.5 % of heat transfer via conduction and radiation heat transfer to conduction heat transfer increases from 1.06 at 350 K to 4.21 % in 900 K. Consequently, in this theoretical modeling, considering heat conduction as a dominant mode of heat transfer does not impose a large inaccuracy.

After validating the assumptions made in thermal modeling, heat flow equation is derived by examining differential equation of the micro-beam of length dx. Under steady-state conditions, resistive power generated in the element is equal to heat conduction out of the element.

$$E_{out} - E_{in} = q_{gen} \tag{6}$$

$$\begin{aligned} -KA \frac{dT}{dx} |_{x+\Delta x} &= -KA \frac{dT}{dx} |_x + q_{gen} \\ \Rightarrow KA \nabla^2 T &= -\rho \cdot J^2, \quad J = \frac{I}{A} \end{aligned} \tag{7}$$

where, J is the current density and ρ is the resistivity.

Since the designed nano-manipulator is for micro-scaled application compatible with the conventional

Table 1 Material property of polysilicon

Physical constant	Value	Notation
Elasticity	169 GPa	E
Poisson ratio	0.22	ν
Resistivity	1.1 e-5 Ω m	ρ
Specific heat	702.24 W/Kg.k	C_p
Heat conduction coefficient	157 W/m.k	K
Thermal expansion	2.5 e-6 1/k	α

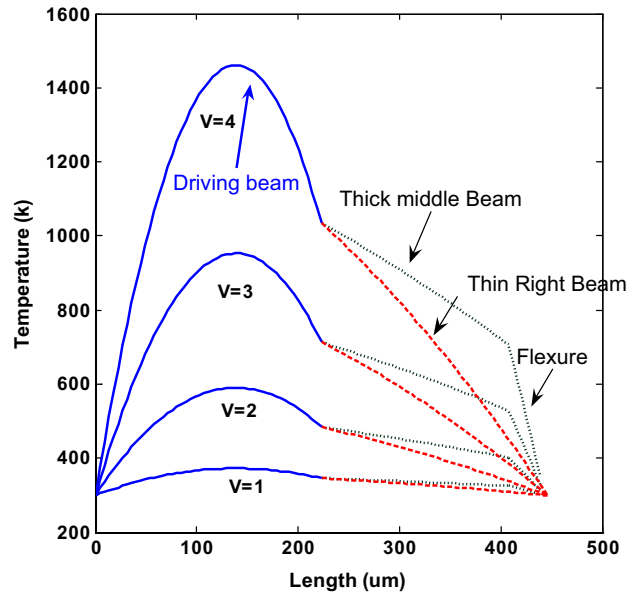


Fig. 5 Temperature distributions in TEMA

micro-fabrication processes, polysilicon is chosen as its material and physical constants of polysilicon used in this analysis are listed in Table 1 (Incorpera and De Witt 2002).

Utilizing continuity of temperature and rate of heat conduction at tip of the actuator and joint part of flexure, temperature distribution in each arm of TEMA is obtained. Temperature profile of the TEMA in its transverse DOF as a function of the applied voltage is plotted in Fig. 5 and Comparison of temperature profiles obtained from analytical and numerical analysis for both DOFs is studied in Fig. 6a, b.

Thermal strain of each micro-beam is then computed as:

$$\begin{aligned} \Delta L_L &= \int_0^L \alpha (T_L(x) - T_0) dx \\ \Delta L_R &= \int_0^L \alpha (T_R(x) - T_0) dx \\ \Delta L_m &= \int_L^{2L-b} \alpha (T_{m1}(x) - T_0) dx + \int_{2L-b}^{2L} \alpha (T_{m2}(x) - T_0) dx \end{aligned} \tag{8}$$

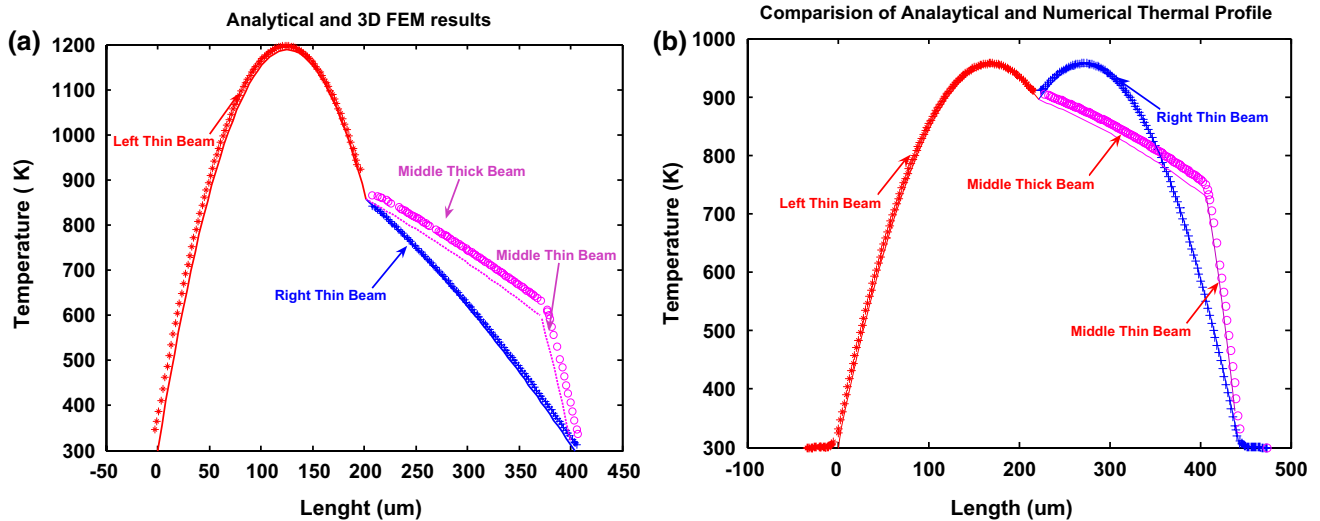
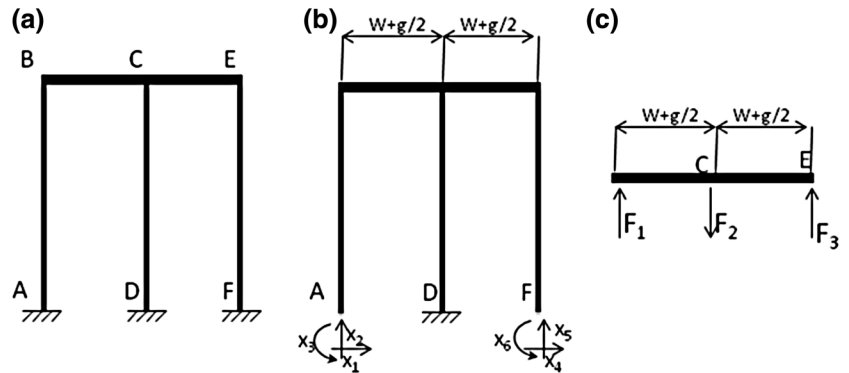


Fig. 6 Comparison of numerical and analytical temperature profile, a transverse DOF, b longitudinal DOF

Fig. 7 Theoretical modeling of TEMA; a transverse DOF, b longitudinal DOF



where, α is the thermal expansion coefficient, T_0 is the room temperature and T_L , T_R , T_{m1} and T_{m2} represent temperature distribution in left, right, middle beam and the flexure respectively.

3.1.3 Structural analysis

Different methods are utilized to obtain range of motion of the actuator performing in each of its DOFs. In the transverse DOF, bending is the dominant mode creating deflection while in the longitudinal DOF, axial force generates motion.

3.1.3.1 Transverse DOF The structure of the thermal actuator is similar to a plane rigid frame with three bases fixed. This structure is statically undetermined with six degrees. To analyze this actuator, first force method is applied to obtain the six redundant of the structure as depicted in Fig. 7b. Then applying unit force method, tip deflection of the actuator is derived.

In force method, stored elastic energy in the structure is first computed as a function of six redundant. Then applying boundary conditions and solving the following simultaneous equations, indeterminacies of the structure are obtained.

$$\begin{bmatrix} f_{11} & f_{12} & \cdots & f_{16} \\ f_{21} & f_{22} & \cdots & f_{26} \\ \vdots & \vdots & \ddots & \vdots \\ f_{61} & f_{62} & \cdots & f_{66} \end{bmatrix} = \begin{bmatrix} \Delta L_L - \Delta L_R \\ 0 \\ \vdots \\ 0 \end{bmatrix} \tag{9}$$

where, $f_{ij} = \frac{\partial U}{\partial X_i \partial X_j}$, U is the stored elastic energy, X_i is the i th redundant and ΔL_L , ΔL_R are thermal strain induced by Joule heating in the left and right micro beams, respectively.

According to the unit force method, virtual work principle (Zbikowsh et al. 1994), tip displacement of the actuator is derived using:

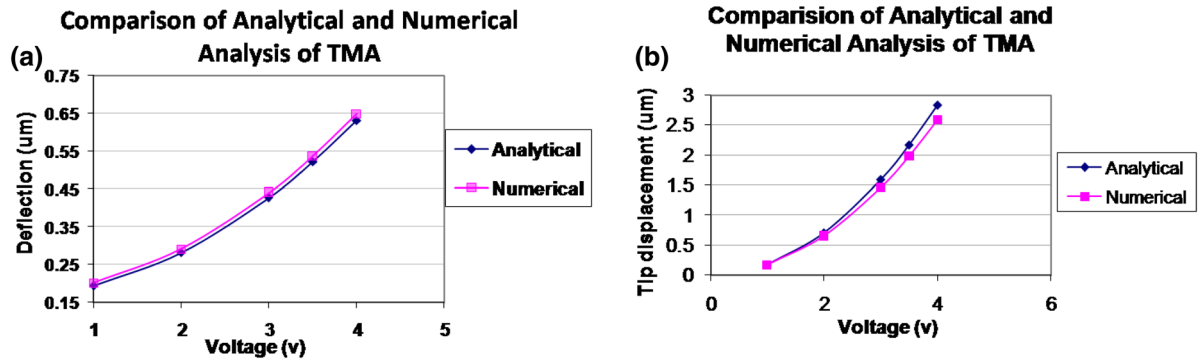


Fig. 8 Comparison of analytical and numerical tip displacement, **a** transverse DOF, **b** longitudinal DOF

$$U_x = \frac{1}{EI_L} \int_0^L (x_3 + x_2 \cdot y) \cdot (L - y) dy \tag{10}$$

3.1.3.2 Longitudinal DOF For the next DOF of the structure another method is applied to obtain tip displacement, since the dominant mode of deflection is axial strain instead of bending (Fig. 6c). Solving compatibility equations and Newton law simultaneously internal forces in the structure is obtained:

$$\begin{aligned} \delta y_B &= \delta y_C = \delta y_E \\ F_1 + F_3 &= F_2 \end{aligned} \tag{11}$$

δy_B , δy_C and δy_E are elastic strains in each arm of the TEMA resulted from combination of thermal strain and axial structural strain. Tip deflection of the TEMA in its longitudinal DOF is then derived from

$$\delta y_C = \Delta L_m + \frac{F_2 (L - b)}{EA_{m1}} + \frac{F_2 b}{EA_{m2}} \tag{12}$$

Comparison of tip displacement derived from analytical and numerical analysis in transverse and longitudinal DOFs are plotted in Fig. 8.

4 Identification of nano-manipulator

Forward and inverse kinematic of the presented nano-manipulator is identified employing neural network concept. For training the system, data sets obtained via FEM solution are used.

Since in this design six actuators are integrated having two separate modes of operation, twelve input parameters exist while six output parameters indicate the stage’s position; $U_x, U_y, U_z, \Theta_x, \Theta_y, \Theta_z$. Hence for forward kinematic, mapping is from the input voltages space R^{12} to the stage positions space R^6 and in reversely for the inverse kinematic mapping is from R^6 to R^{12} . From the classical mathematical theorem it is known that.

Theorem 1 For any continuous mapping $f: R^n \rightarrow R^m$, there must exist a three-layer neural network having an input layer with n processing elements, a hidden layer with $(2n + 1)$ processing elements, and an output layer with m processing elements that implement f exactly (Zbikowsh et al. 1994).

This theorem shows that neural networks can approximate any function in the real world. For identification of the nano-manipulator since the position of the stage is a continuous function of the input voltages, a three layer neural network is used. More layers introduce more freedom but greatly increase complexity and reduce convergence rate. Then following the detailed universal approximator in Theorem 2 activation functions are chosen.

Theorem 2 For any continuous mapping $f: R^n \rightarrow R^m$ and any positive real number ϵ there exist sigmoidal functions \mathfrak{S} and staircase-like function $x_i, \varphi_{ij} \in S(\mathfrak{S})$ such that for every (x_1, x_2, \dots, x_n) .

$$\left| f(x_1, x_2, \dots, x_n) - \sum_{i=1}^k x_i \left(\sum_{j=1}^n \varphi_{ij}(x_j) \right) \right| < \epsilon \tag{13}$$

where $S(\mathfrak{S})$ is a set of functions in the form of $\sum_{i=1}^k a_i \sigma(b_i x + c_i)$. Thus a hyperbolic tangent sigmoid transfer function is selected as the activation function of this neural network. Figure 9 depicts a schematic of the neural network utilized for identification of the forward kinematic; A three layer neural network with 12 neurons in the input layer, 25 neurons in the hidden layer and 6 neurons in the output layer and two hyperbolic tangent sigmoid functions and a pure linear function for the output layer.

In order to verify performance of the neural network, four data sets gained from FEM solution were put aside while training the network. Figures 10 and 11 indicate stage’s translational and rotational positions due to the applied input voltages once obtained from the FEM solution and once from the trained neural network. As clarified in the following figures precise estimation of positioning of

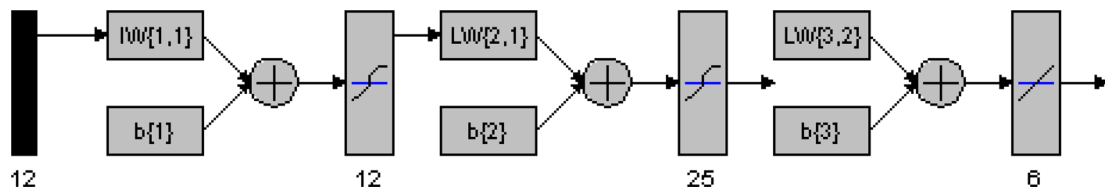


Fig. 9 Schematic of the neural network used in forward kinematic identification of the nanomanipulator

Fig. 10 Performance study of neural network in identifying translational outputs of the nanomanipulator

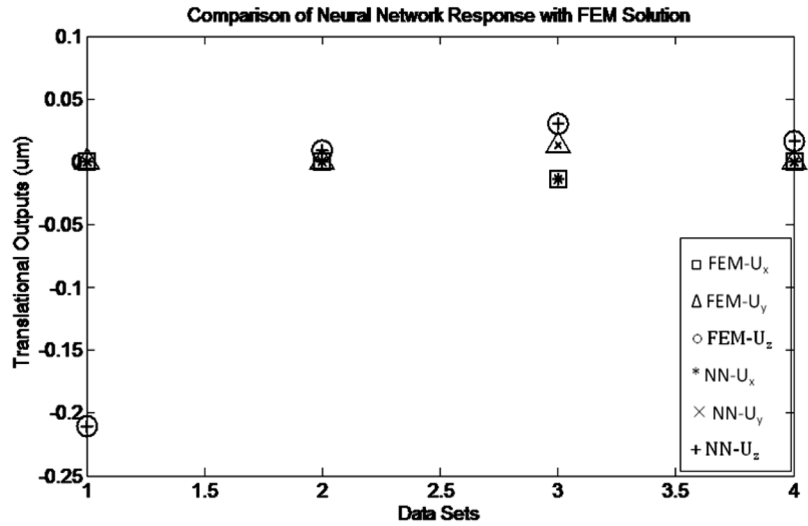
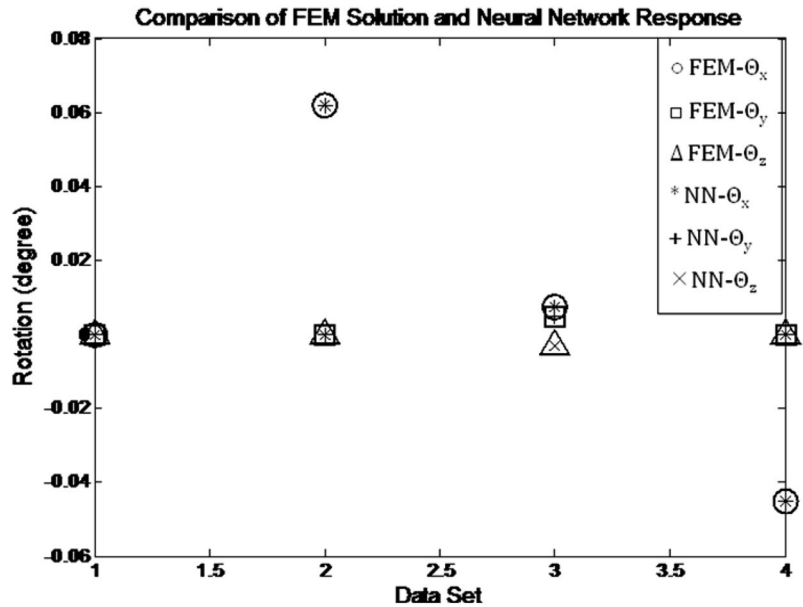


Fig. 11 Performance study of neural network in identifying rotational outputs of the nanomanipulator

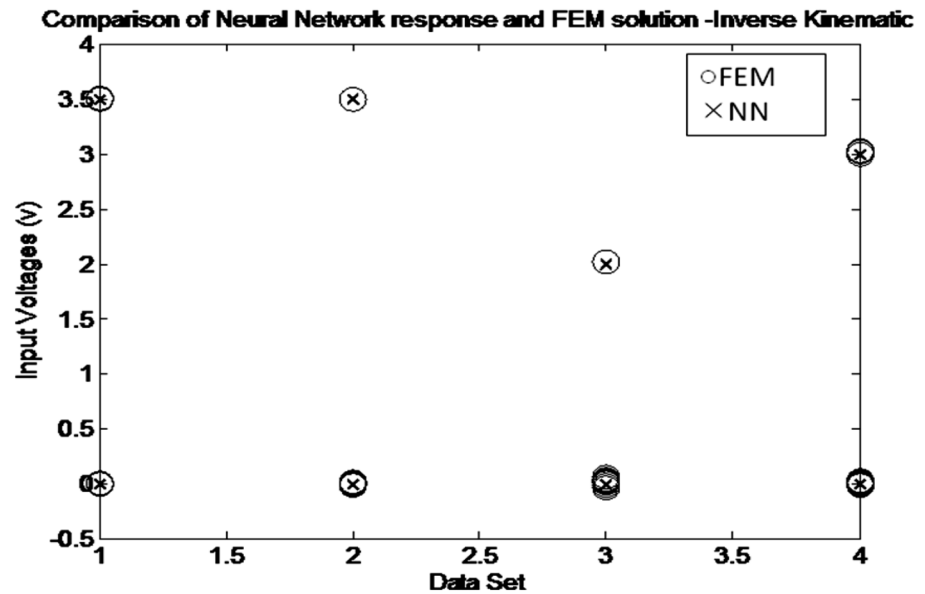


the stage is done using a well trained neural network that can replace time-consuming analytical or numerical solutions or expensive experimental setups.

Similarly for identification of the inverse kinematic of the nano-manipulator a three layer network with hyperbolic

tangent sigmoid activation functions is trained in order to obtain the voltages required to be applied to the base of the actuators for reaching a desired stage position. Figure 11 demonstrates the agreement between the neural network response and the FEM solution.

Fig. 12 Performance of neural network in inverse kinematic identification of the nanomanipulator



As it is clear in Fig. 12, neural network is beneficial in identification of the inverse kinematic giving us a method to obtain what arrangement of voltages are required to displace the center stage to a desired position.

5 Conclusion

A novel micro-scale nanopositioner capable of positioning in all six degrees of freedom was designed. Since rigid-link mechanisms with traditional joints cannot be extended to micro scale applications and are not able to achieve sub micron accuracy, compliant mechanism concept comprising of flexure hinges was opted for designing the nanopositioner. In flexure hinge mechanisms, friction, backlash and wear are eliminated increasing its accuracy. In addition, the monolithic pattern of the compliant mechanism has simplified its production by conventional micro-fabrication processes.

References

- Chen WC, Chu CC, Hsieh J, Fang W (2003) A reliable single layer out of plane micromachined thermal actuator. *Sens Actuators A* 103:48–53
- Chen SC, Culpepper ML (2006) Design of a six-axis micro-scale nanopositioner- μ HexFlex. *Precis Eng* 30:314–324
- Chen SC (2003) A six-degree-of-freedom compliant micro-manipulator for silicon optical bench. M.S. Thesis, Massachusetts Institute of Technology
- Culpepper ML, Anderson G (2004) Design of a low-cost nano-manipulator which utilizes a monolithic, spatial compliant mechanism. *Precis Eng* 28:469–482
- Dash JN, Jha R, Villatoro J, Dass S (2015) Nano-displacement sensor based on photonic crystal fiber modal interferometer. *Opt Lett* 40:467–470
- Hosseini N, Nievergelt AP, Adams JD, Stavrov VT, Fantner GE (2016) A monolithic MEMS position sensor for closed-loop high-speed atomic force microscopy. *Nanotechnology* 27:135705
- Incorpera FP, De Witt DP (2002) Introduction to heat transfer, 4th edn. Wiley, New York, pp 239–271
- Lai Y, Kujath M, Hubbard T (2005) Modal simulation and testing of a micro-manipulator. *J Dyn Syst Meas Contr* 127:515–519
- Moulton T, Ananthasuresh GK (2001) Micromechanical devices with embedded electro-thermal compliant actuators. *Sens Actuators A* 90:38–48
- Rubio-Sierra FJ, Heckl WM, Stark RW (2005) Nanomanipulation by atomic force microscopy. *Adv Eng Mater* 7:193–196
- Sitti M, Hashimoto H (2000) Controlled pushing of nanoparticles: modeling and experiments. *IEEE/ASME Trans Mechatron* 5:199–211
- Sutherland J et al (1995) Optical coupling and alignment tolerances in optoelectronic array interface assemblies. *IEEE electronic components and technology conference*
- Trease BP, Moon YM, Kota S (2005) Design of large displacement compliant joints. *Trans ASME* 127:788–798
- Yao Q, Dong J, Ferreira PM (2007) Design, analysis, fabrication and testing of a parallel-kinematic micropositioning XY stage. *Int J Mach Tools Manuf* 47:946–961
- Zbikowsh R et al (1994) A review of advances in neural adaptive control systems. NACT technical report 8039